Archives of Materials Science and Engineering

Volume 114
Issue 1
March 2022
Pages 13-23

International Scientific Journal published monthly by the World Academy of Materials and Manufacturing Engineering

DOI: 10.5604/01.3001.0015.9848

Characteristics of polymer ring springs

G. Wróbel
Department of Theoretical and Applied Mechanics, Mechanical Engineering Faculty, Silesian University of Technology, ul. Konarskiego 18a, 44-100 Gliwice, Poland
Corresponding e-mail address: gabriel.wrobel@polsl.pl
ORCID identifier: https://orcid.org/0000-0002-7704-2466

ABSTRACT

Purpose: The paper discusses selected aspects of the use of polymeric materials in the construction of ring springs.

Design/methodology/approach: Special attention is paid to differences in characteristics of such materials in comparison to springs made of traditional material - steel.

Findings: The result of the work is a static-dynamic model of polymer ring springs. An analysis of the influence of friction on the performance characteristics was carried out. The results of the preliminary experimental studies confirm the correctness of the model.

Practical implications: Analytical models have been developed, as tools to support the design processes of ring spring structures, in the field of innovative material solutions. They are a tool for the selection of geometric and material characteristics of springs, meeting the set operational expectations.

Originality/value: Extensive possibilities in the selection among a group of structural polymer materials allow the formation of structural solutions with a variety of characteristics, both elastic and impact or damping. The area of application ranges from mechanical engineering to construction or transportation. The characteristics complement the possible field of solutions in cases of use of traditional metallic materials, especially high-grade steels. Material solutions make it possible to achieve significant economic effects in addition to unavailable performance characteristics, both static and dynamic. These are due to competitive prices for polymer materials, including composites, and manufacturing costs. They open up a wide field for utility innovations.

Keywords: Ring springs, Polymer materials, Geometric features, Design, Mechanical characteristics, Friction

Reference to this paper should be given in the following way:

G. Wróbel, Characteristics of polymer ring springs, Archives of Materials Science and Engineering 114/1 (2022) 13-23. DOI: https://doi.org/10.5604/01.3001.0015.9848

METHODOLOGY OF RESEARCH, ANALYSIS AND MODELLING

1. Introduction

Springs, in mechanical engineering, are structural elements whose essential characteristic, used in both static and dynamic systems, is their elasticity [1-3]. This feature describes the relationship between the deformation of an element and its load. In the simplest case, this relationship is linear – the strain is proportional to the load.

$$q = k \cdot Q \tag{1}$$

© Copyright by International OCSCO World Press. All rights reserved. 2022

where: q – generalized strain, Q – generalized force, k – elastic element stiffness.

Stiffness is sometimes dependent on strain, strain rate, or temperature. This means nonlinear elasticity. Perfectly elastic elements have the ability to return to their original state after the load is removed.

Generalized deformation is often a simple deformation of compression, tension, bending, or torsion, but the load can be complex. The deformed material can be an elastic construction element or a gas. Liquids are unlikely to be suitable due to their low compressibility.

In terms of loads nature, we can distinguish constants, such as in tensioning or pressure elements, steppers, as in fender elements, variables, as in measuring instruments or clocks, fatigue, in the case of repetitive work cycles.

Popular types of springs are helical, spiral, flat, disc, and ring in terms of form. In terms of material – metal, polymer, composite. In special cases, they can also be produced from natural resources, e.g., furniture or musical instruments.

The basic functional characteristics are related, in addition to the nature of the load, with the range of utility values of loads and deformations, boundary loads, and the stiffness variability function. These requirements determine the selection of the right spring element. In this respect, loads are divided into static and dynamic [4-6].

An inevitable effect of spring deformation is the dissipation of energy into friction, heat, or structural changes in the material. This applies to work under conditions of variable dynamic loads. The energy dissipation is related to the hysteresis of the strain function. Many components, referred to as springs, use the energy dissipation effect to damp or cushion systems. The design of such elements requires considering both the static and dynamic load conditions and the damping characteristics.

Each of the spring structural classes gives the possibility to determine design parameters, the selection of which may be the subject of optimization.

2. Spring rings

One of the listed classes of springs construction is ring springs. Their general form is shown in Figure 1 [7]. These springs can bear compressive loads, which is conditioned by one-sided axial displacement constraints.

Such springs consist of inner and outer rings, the cross-sections of which should be the same due to their close to equivalent operating conditions. The principle of elastic axial deformation of an element is based on the relationship of mutual loads on the contact surfaces of the rings with changes in their diameters, which results in their mutual slip, the size of which is determined by a relative change in diameters. Due to the repeatability of the load and deformation conditions for successive ring spring modules (Fig. 2), loads of the outer rings can be considered the same with the accuracy of local deviations. The same applies to the inner rings. However, they differ because the outer rings are stretched, and the inner rings are compressed. By changing the number of elements, the deflection of the spring, and therefore its stiffness, can be adjusted. The serial connection of individual rings makes their loads and deformations equal, except for the end half rings, the load and deformation state of which depends on the method of support. Similar load and deformation states can also be structurally provided to the end elements employing an appropriate fixing method. Due to the repeatability of the load states of individual spring modules, the range of permissible spring loads does not depend on the number of modules and, therefore, the number of rings. The maximum load for a different number of spring elements is constant, while the maximum deflection of the spring and its length vary.

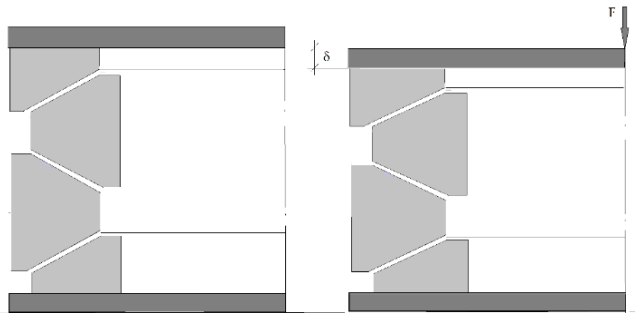

Fig. 1. Spring ring structural form

The aforementioned design features of the coil springs enable achieving a variety of performance characteristics, including the elastic stiffness of the elements and the degree of deformation energy dissipation. The quantitative measures of these characteristics depend on the geometrical features of the elements, such as the diameters of the rings, the dimensions of the cross-sections, and the number of elastic modules. Equally important are the material characteristics of the components, which are essential both for the stiffness of the spring and its damping capacity.

The following sections will analyse:

an elastic model, the conclusions of which will be used to assess the effect of the dimensions of the ring cross-section on the spring stiffness;

the influence of the ring material on the spring characteristics.

Independently, an analysis of the influence of friction on the stiffness and damping capacity of the spring will be carried out, as well as a discussion of the importance of lubrication – element cooling.

3. Analysis of the load condition of ring springs in the linear-elastic range, without friction

The linear range of deformation corresponds to the elastic deformation of the rings in the analysed load range while neglecting the friction that occurs on the conical surfaces of the rings. Figure 2 shows the spring modulus adopted for the analysis as a repetitive set of half-rings in contact.

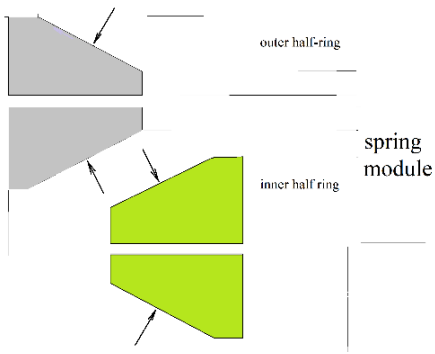

Fig. 2. Diagram of the half-ring system with marked mutual pressure forces

Figure 3 shows the cross-sectional figures of the symmetrical parts of the inner and outer rings.

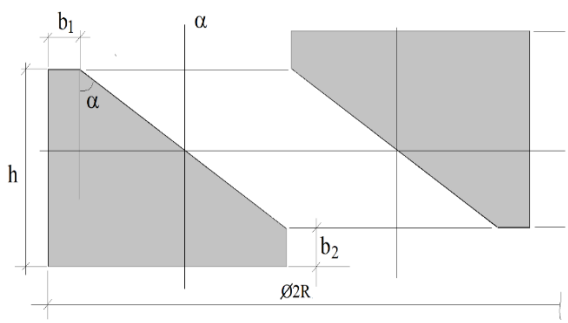

Fig. 3. Figures of symmetrical sections of the inner and outer ring parts

Figure 4 shows the symmetrical part of the outer ring cross-section, with marked reduced load components resulting from the interaction on the contact surface of the inner ring in the case of spring compression. The lack of friction means the absence of the tangential component of the interaction between the rings. It is assumed that the shown loads represent the intensities of the linear loads distributed along the circumference of the ring.

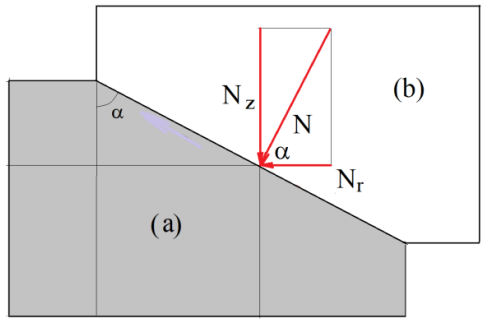

Fig. 4. Symmetrical part of the outer section (a) and inner (b) ring, with reduced load components marked

Thus, the axial load force F of the spring corresponds to the mutual ring pressure N_z, distributed axially-symmetrically on the ring contact surface, with the intensity of the axial component equal to:

$$N_z = \frac{F}{2\pi R} \tag{2}$$

It induces a reciprocal pressure between the rings along the line of a circle of radius R, located at the midpoint of the conical contact surface with an intensity:

$$N = \frac{N_z}{\sin\alpha} \tag{3}$$
$$N = \frac{F}{(2\pi R \sin\alpha)}$$

Intensity of the radial component:

$$N_r = N_z \cot\alpha \tag{4}$$

causes the outer ring to stretch by a force:

$$S_z = RN_r \tag{5}$$
$$S_z = \frac{F\cot\alpha}{2\pi}$$

Figure 5 shows the ring load with the circumferential tensile forces S_z marked.

The axial stiffness of the spring module depends on:
the opening angle of the conical surface 2α;
the cross-sectional figures of the inner and outer rings, defined by the dimensions h and b;
the materials of outer and inner rings.

For the tensile stiffness of the outer ring $k_r = EA$, the ring tensile force S increases the ring radius by

$$\delta R_z = \frac{RS_z}{EA} \qquad (6)$$
$$\delta R_z = \frac{RF\cot\alpha}{2\pi EA}$$

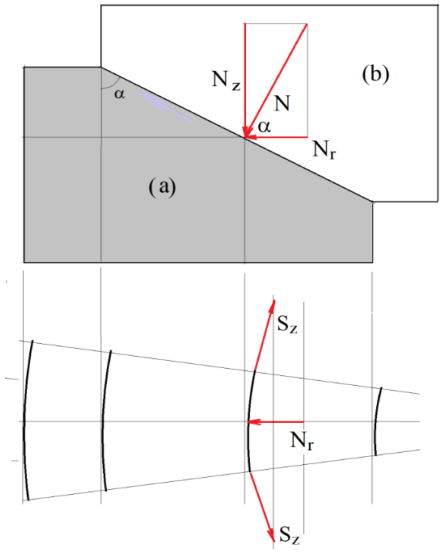

Fig. 5. Load system for the ring section with circumferential tensile forces S_z marked

A similar analysis of the loads on the inner ring, marked with the letter (a) in Figure 6, shows that the mutual pressure component of the rings N_r differs only in sign, which means compression of the inner ring.

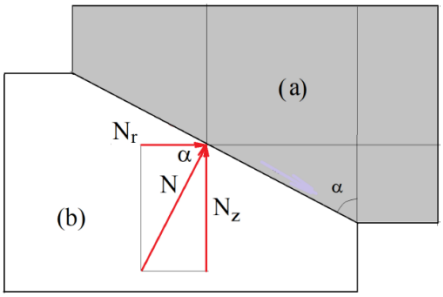

Fig. 6. Symmetrical part of the section of the inner ring (a), with the reduced load components marked

The circumferential force S_w has the value:

$$S_w = \frac{F\cot\alpha}{2\pi} \qquad (7)$$

For the compressive stiffness of the inner ring $k_c = EA$, the compressive force on the ring decreases the radius by:

$$\delta R_w = -\frac{RS_w}{EA} \qquad (8)$$

$$\delta R_w = -\frac{RF\cot\alpha}{2\pi EA}$$

Figure 7 shows the change in the relative position of the rings in the section of the analysed spring module. The distances R_z and R_w marked in Figure 7, for the adopted assumptions, differ only in signs, in accordance with formulas (6) and (8).

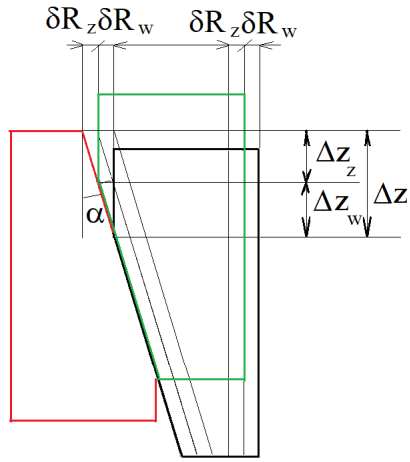

Fig. 7. Change of relative ring position in cross-section of the analysed spring module

Corresponding changes in the relative axial position of the rings:

$$\Delta z_z = \delta R_z \tan\alpha$$
$$\Delta z_z = \frac{RF}{2\pi EA}$$
$$\Delta z_w = -\frac{RF}{2\pi EA}$$
$$\Delta z = \Delta z_z - \Delta z_w$$
$$\Delta z = \frac{RF}{\pi EA} \qquad (9)$$

Hence the stiffness of one spring module:

$$K^{(1)} = \frac{F}{\Delta z}$$
$$K^{(1)} = K^{(1)} = \frac{(\pi EA)}{R} \qquad (10)$$

The stiffness of a spring composed of n modules, which means (n-1) full rings and two marginal half rings, will be:

$$K^{(n)} = K^{(1)} = \frac{(\pi EA)}{nR} \qquad (11)$$

The lack of friction means that the dependence of the spring deflection on the axial force value remains the same for compression as for tension. The initial value F_1 corresponds to the preload of the spring. The interval (Z_1, Z_2) is the operating range. Suppose the spring load source is a constant weight of supported mass, with initial kinetic energy E_k. In that case, the deflection changes have the

character of harmonic vibrations, with an amplitude depending on the system energy. Its total value is equal to

$$E = E_{k1} + U_1 = U_S + U_2 \tag{12}$$

where E_{k1} – initial kinetic energy of the sprung mass, U_1 – initial potential energy of the mass position, U_S – final spring deformation energy, U_2 – final mass potential energy. The positional energy difference can generally be neglected.

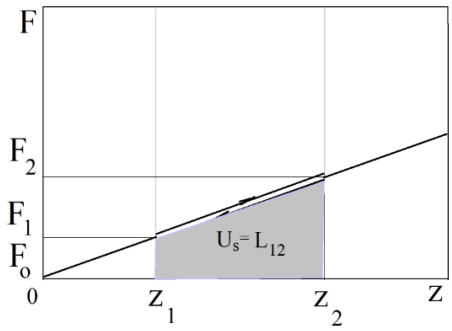

Fig. 8. Dependence of the spring deflection on the value of axial force without taking friction into account

The change of elastic energy of the deformed spring for deflection z is

$$U_S = L_{12} = \left(\frac{1}{2}\right)(z_2F_2 - z_1F_1) \tag{13}$$

and is equal to the compressive force $F_{(z)}$ work on the compression path. This is illustrated in Figure 8.

4. Analysis of the load condition of ring springs in the linear-elastic range, taking into account friction

In this model of ring springs, the linear elastic deformation of the rings is maintained while taking into account the friction on the conical surfaces of the mutual pressure of the rings. A dry friction model will be adopted, in which the frictional force on the conical surfaces of the rings is proportional to the mutual pressure force of the rings on the conical contact surfaces. The load condition in compression and tension of the spring requires a separate analysis.

4.1. Spring compression

Figure 9 shows cross-sections of the cooperating half-rings: the outer ring and the inner ring. On the edge of the conical slip surface of the rings, the circumferential load vectors with the axial force N_z and the components resulting from its distribution are marked: N – perpendicular to the contact surface, T – friction force, their resultant N' and radial component N_r. They correspond to the load intensity distributed linearly on the central circle of the conical contact surface. The load proportions result from the assumed friction angle, causing a change in the contact force N' direction. The sliding friction coefficient μ is defined by the relation $\tan\beta = \mu$. The presented friction force orientation corresponds to the compression phase of the spring.

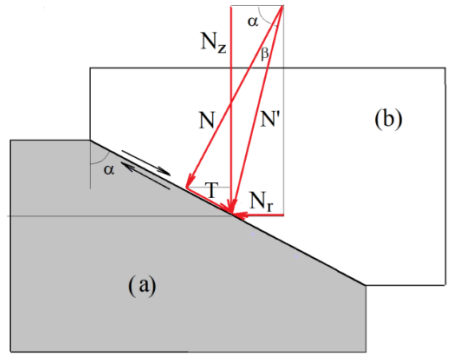

Fig. 9. Load distribution of the outer (a) inner (b) half ring, taking into account friction, in the case of compression

Similarly to formulas (6) and (8), for the assumed dimensions of the rings, their only differing in sign deformations determine the changes in the radius:

$$\delta R_z = \frac{RS_z}{EA}$$
$$\delta R_w = -\frac{RS_w}{EA} \tag{14}$$

The circumferential forces in the rings will change. The frictional force T appears in the system of forces loading the outer ring:

$$T = N\tan\beta \tag{15}$$

Subsequent dependencies lead to the determination of the relationship between the axial load force of the spring $F^{(s)}$ and the tensile force of the outer ring S_z.

$$N_r = N'\sin\left(\frac{\pi}{2} - (\alpha + \beta)\right)$$

$$N_r = N'\cos(\alpha + \beta) \tag{16.1}$$

$$N' = \frac{N}{\cos\beta} \tag{16.2}$$

$$N_z = N\sin\alpha + T\cos\beta$$
$$N_z = N(\sin\alpha + \tan\beta\cos\alpha) \tag{16.3}$$

$$N = \frac{N_z}{(\sin\alpha + \tan\beta\cos\alpha)} \tag{16.4}$$

$$N' = \frac{N_z}{(\sin\alpha + \tan\beta\cos\alpha)\cos\beta} \tag{16.5}$$

$$N_r = \frac{N_z\cos(\alpha+\beta)}{(\sin\alpha + \tan\beta\cos\alpha)\cos\beta} \tag{16.6}$$

$$N_r = \frac{F^{(s)}\cos(\alpha+\beta)}{2\pi R(\sin\alpha + \tan\beta\cos\alpha)\cos\beta} \tag{17}$$

It can be noted that the radial component of N_r for friction angle $\beta = 0$ takes the value:

$$N_r = N_z\cot\alpha \tag{18}$$

which is consistent with equation (4).

The tensile force of the ring is equal to:

$$S_z = RN_r$$

$$S_z = \frac{F^{(s)}\cos(\alpha+\beta)}{2\pi(\sin\alpha + \tan\beta\cos\alpha)\cos\beta} \tag{19}$$

Hence the change in the radius of the outer ring:

$$\delta R_z = \frac{RS_z}{EA}$$

$$\delta R_z = \frac{RF^{(s)}\cos(\alpha+\beta)}{2\pi EA(\sin\alpha + \tan\beta\cos\alpha)\cos\beta} \tag{20}$$

The load on the inner ring will be opposite to that specified for the outer ring, so also the change in radius will differ only in sign:

$$\delta R_w = \frac{-RF^{(s)}\cos(\alpha+\beta)}{2\pi EA(\sin\alpha + \tan\beta\cos\alpha)\cos\beta} \tag{21}$$

Accordingly, analogous to formula (9), there will be a relative axial displacement of the rings:

$$\Delta z = \Delta z_z - \Delta z_w$$

$$\Delta z = \frac{RF^{(s)}\cos(\alpha+\beta)\tan\alpha}{\pi EA(\sin\alpha + \tan\beta\cos\alpha)\cos\beta} \tag{22}$$

Hence the stiffness of one spring module:

$$K^{(1)} = \frac{\pi EA(\sin\alpha + \tan\beta\cos\alpha)\cos\beta}{R\cos(\alpha+\beta)\tan\alpha} \tag{23}$$

The stiffness of a spring composed of n modules, which means (n-1) solid rings and two marginal half rings, will be:

$$K^{(n)} = \frac{\pi EA(\sin\alpha + \tan\beta\cos\alpha)\cos\beta}{nR\cos(\alpha+\beta)\tan\alpha} \tag{24.1}$$

for $\beta = 0$

$$K^{(n)} = \frac{(\pi EA)}{nR} \tag{24.2}$$

which is consistent with formula (11).

The plot of the dependence $F_{(z)}$ is, as in the case of the frictionless system, a line graph, which is shown on the line (1-2) in Figure 10. The initial value of F_{1Z} corresponds to the axial component of the force under friction between the rings. The work of friction forces within the range of spring deflections corresponds to the diagram's shaded area (1-2-3-4) (Fig. 10).

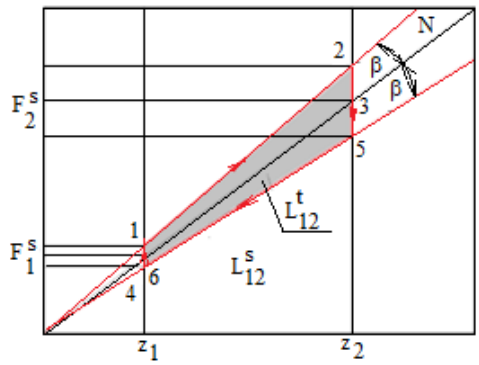

Fig. 10. Work and energy associated with the deflection of the spring in the compression and tension phases, taking friction into account

The work of spring deformation for the deflection Δz is

$$L'_{12}$$

$$L'_{12} = \left(\frac{1}{2}\right)(z_2F_2^s - z_1F_1^s)$$

$$L_{12} = L_{12}^S + L_{12}^T$$

$$L_{12}^T = 0{,}5(F_2^s + F_1^s)\tan\beta \tag{25}$$

The work L_{12} is equal to the initial energy of the amortized mass – the area under the force diagram (1-2) (Fig. 10). In the end position z_2, the elastic deformation energy reaches the value L^S_{12}, which corresponds to the area under the line (3-4), while the remaining part (1-2-3-4) is the energy converted into heat due to friction, associated with the performance of frictional work L^T_{12} during compression – the darker part, with the value

$$L_{12}^T = F_0\Delta z \tag{26}$$

4.2. Spring expansion

The state of load on the rings during the spring expansion phase is different, as evidenced by the change in the sign of the friction force (Fig. 11).

The important dependencies (14) remain. The circumferential forces in the rings determined by equation (17), and the resulting deformation, which is measured by changes in the radius of the rings, will change, according to equations (19) and (20). This is caused by the inversion of the friction force vector T.

$$T = N\tan\beta \tag{27}$$

Subsequent dependencies lead to the determination of the relationship between the force of the axial load of the spring $F^{(r)}$ and the tensile force of the outer ring S_z (Fig. 11).

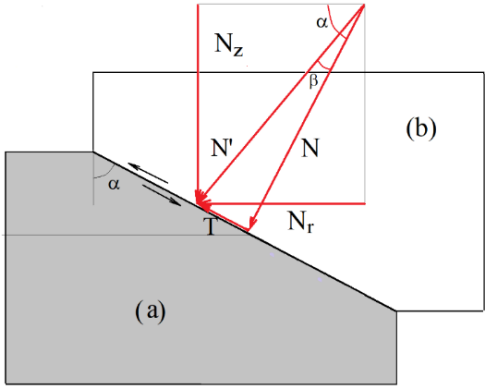

Fig. 11. Load distribution of the outer (a) inner (b) half-ring, including friction, in the case of expansion

$$N_r = N' \cos(\pi - \beta - \pi + \alpha)$$
$$N_r = N' \cos(\alpha - \beta) \tag{28.1}$$

$$N' = \frac{N}{\cos\beta} \tag{28.2}$$

$$N_z = N \sin\alpha - T \cos\alpha$$
$$N_z = N(\sin\alpha - \tan\beta \cos\alpha) \tag{28.3}$$

$$N = \frac{N_z}{(\sin\alpha - \tan\beta \cos\alpha)} \tag{28.4}$$

$$N' = \frac{N_z}{(\sin\alpha - \tan\beta \cos\alpha)\cos\beta} \tag{28.5}$$

$$N_r = \frac{N_z \cos(\alpha-\beta)}{(\sin\alpha - \tan\beta \cos\alpha)\cos\beta}$$
$$N_r = \frac{F^{(r)} \cos(\alpha-\beta)}{2\pi R(\sin\alpha - \tan\beta \cos\alpha)\cos\beta} \tag{29}$$

It can be noted that the radial component of N_r for friction angle = 0 takes the value

$$N_r = N_z \cot\alpha \tag{30}$$

which is consistent with equation (4).

The tensile force of the ring is:

$$S_z = RN_r$$
$$S_z = \frac{F^{(r)} \cos(\alpha-\beta)}{2\pi(\sin\alpha - \tan\beta \cos\alpha)\cos\beta} \tag{31}$$

Hence the change in the radius of the outer ring:

$$\delta R_z = \frac{RS_z}{EA}$$
$$\delta R_z = \frac{RF^{(r)} \cos(\alpha-\beta)}{2\pi EA(\sin\alpha \tan\beta \cos\alpha)\cos\beta} \tag{32}$$

The load on the inner ring will be opposite to that specified for the outer ring, so also the change in radius will differ only in sign:

$$\delta R_w = \frac{RF^{(s)} \cos(\alpha-\beta)}{2\pi EA(\sin\alpha - \tan\beta \cos\alpha)\cos\beta} \tag{33}$$

Accordingly, analogically to equation (8), there will be a relative axial displacement of the rings:

$$\Delta z = \Delta z_z - \Delta z_w$$
$$\Delta z = \frac{RF^{(r)} \cos(\alpha-\beta)\tan\alpha}{\pi EA(\sin\alpha \tan\beta \cos\alpha)\cos\beta} \tag{34.1}$$

for $\beta = 0$

$$\Delta z = \frac{RF^{(r)}}{\pi EA}$$

which is consistent with formula (9).

In the position of the greatest deflection of the spring, the conditions change from compression to tension. This change is accompanied by a change in the sign of the friction force. In the intermediate state, in which the friction force takes the value of zero, the contact force, corresponding to the equilibrium state in the achieved deformation state, will be equal to the force in the frictionless system

$$F^{(r)} = \frac{\pi EA\Delta z}{R} \tag{35}$$

and then in equation (22), corresponding to the largest deflection in the compression phase, the plus signs are changed to minus signs. This represents a change in the compressive force of the spring by F, enabling the return movement:

$$\Delta F = 2\pi RN[(\sin\alpha \tan\beta \cos\alpha) - (\sin\alpha - \tan\beta \cos\alpha)]$$
$$\Delta F = 4\pi RN \tan\beta \cos\alpha \tag{36}$$

The magnitude of the jump in force value increases as the friction coefficient and the cone angle of the ring's contact surface increase.

The changes in the force value F, depending on the spring deformation, in the conditions of transition from the compression to the expansion phase are shown in Figure 10. The part (3-5-6-4) of the dark field measures the energy dissipated by the L^T_{21} friction during the spring unloading. Under the line (5-6), the remaining part of the field corresponds to the part of the elastic energy retained after one working cycle.

The work of deformation of the spring L^S_{34}, corresponding to the elastic energy, is negative in this phase, reducing the elastic energy in the compressed state L^S_{12} to zero, the case of the spring returning to its initial dimension. Simultaneously, the work of friction is performed – the dark field of the filling. The work of spring relaxation, for deflection z, is L^S_{34} and differs only in sign from the work L'_{43} – it is negative. The total work in the relaxation phase will be $L_{34} = L^S_{34} + L^T_{34}$

$$L_{34} = L^S_{34} + L^T_{34}$$
$$L^S_{34} = \left(\frac{1}{2}\right)(z_1 F^S_1 - z_2 F^S_2) \tag{37}$$

$$L_{12}^{T} = \left(\frac{1}{2}\right)(F_2^S - F_1^S)\tan\beta\Delta z \quad (38)$$

The total friction work during the spring working cycle is the sum of equal work for compression and expansion and is equal to:

$$L_{14}^{T} = L_{12}^{T} + L_{34}^{T} = (F_2^S + F_1^S)\tan\beta\Delta z \quad (39)$$

5. Damped vibrations of ring springs

As stated in Section 4, the process of spring deformation is accompanied by the execution of work by the spring compression forces, originating from the pressure of the system being damped, associated with the periodic conversion of its kinetic energy E_{k1} into elastic energy and frictional work:

$$L_{12} = \left(\frac{k}{2}\right)(1+\mu)(z_2^2 - z_1^2) \quad (40)$$

$$U_{12} = \left(\frac{k}{2}\right)(z_2^2 - z_1^2) \quad (41)$$

$$L_{12}^{T} = \left(\frac{\mu k}{2}\right)(z_2^2 - z_1^2) \quad .(42)$$

Part of this work increases the elastic energy of the spring deformation, the remaining is related to the work of friction, which is converted into heat.

In the return motion, the elastic energy U_{12} of the spring deformation, achieved in the compression phase, is reduced by a part corresponding to the work of friction force, equal to that done during the expansion (area 3-5-6-4 in Fig. 10). The initial kinetic energy E_{k1} of the cushioned mass is reduced by the total friction work of the first cycle:

$$E_{k2} = E_{k1} - L^T \quad (43)$$

$$L_{34}^{T} = L_{12}^{T} = \frac{\mu k}{2(z_2^2 - z_1^2)}$$

$$L^T = L_{12}^{T} + L_{34}^{T} = \left(\frac{k}{2}\right)[(1+\mu)(z_2^2 - z_1^2) + (1-\mu)(z_1^2 - z_2^2)]$$

$$L^T = \mu k(z_2^2 - z_1^2) \quad (44)$$

As follows, the contribution of friction work (37) to the total compression energy of the spring is:

$$\frac{L^T}{L_{12}} = \frac{k\mu(z_2^2 - z_1^2)}{\frac{1}{2}k(1+\mu)(z_2^2 - z_1^2)} = \frac{2\mu}{(1+\mu)} \quad (45)$$

The remaining kinetic energy E_{k2} can, while remaining in the system, be transformed again in the next spring cycle. In this case, the friction work (field 1-2-5-6) from the first cycle will diminish the energy required for compression in the second cycle. This corresponds to the equality of fields (1-2-5-6) and (2'-2-z2-z'2) (Fig. 12). The circle (1-2'-5'-6) determines the course of the spring deflection in the second cycle. The coordinate *z'2* determines the maximum deflection of the spring.

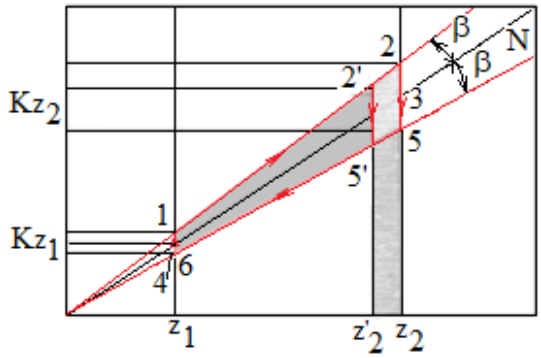

Fig. 12. Two cycles of the spring deflection

In case of such a process the further course of the spring deflection is presented in Figure 13. The motion of the cushioned body has the character of damped oscillations with decreasing amplitude.

In general, the equation of motion has the form in simplified form, with the mass of the spring ignored:

$$m\ddot{z} + T(z) = F(z,t) \quad (46)$$

where m – the cushioned mass, $T(z) = \mathrm{zK}(z)$ – the stiffness of the spring, $F(z,t)$ – the general form of the force, which, for example, for the preload of the spring, as in the previously shown diagrams, will take a constant value.

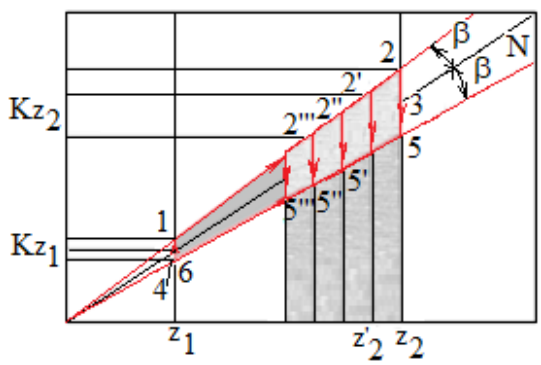

Fig. 13. Vibrations of a system with weak friction damping

The stiffness *K(z)* of the spring, as the amplitude decreases, decreases, so the period of successive cycles will increase. Nonlinearity of spring stiffness also causes nonlinearity of friction forces *T(z)*. Hence, the decrement of damping, used as a characteristic of damped vibrations, is impossible to determine in view of the changing ratio of successive amplitudes of quenching vibrations.

Depending on the value of the damping ratio, the vibrations may have the character of weakly damped vibrations – there is cyclic oscillation with decreasing

amplitude of deflection (Fig. 13). In the critical case, the spring only returns to its initial position (Fig. 14). All energy is dissipated in one cycle of deflection.

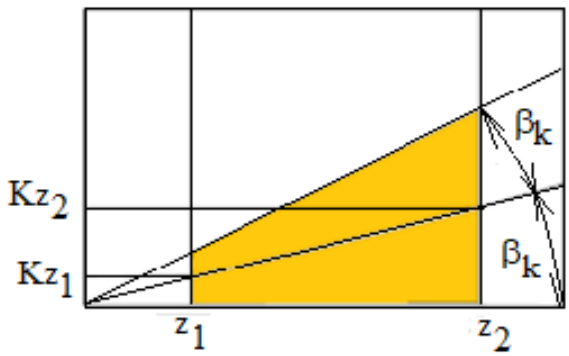

Fig. 14. Critical course of the spring deformation

In the supercritical case the motion stops before returning to the initial position (Fig. 15). Such a case can be referred to as a spring jam, from which extrication requires a force that overcomes the friction forces. The marked areas in Figure 15 (1) and (2) are equal.

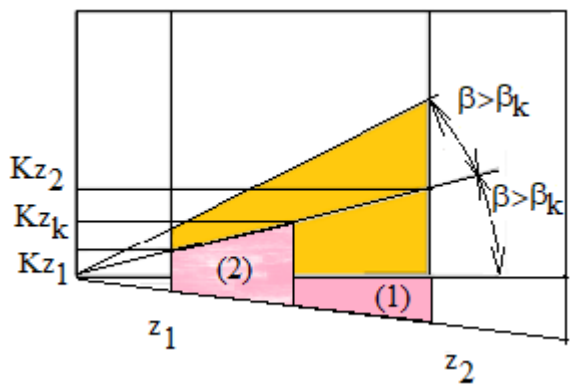

Fig. 15. Supercritical case – motion stops before returning to initial position

In extreme cases the return will not occur (Fig. 16). The deformation is only due to the initial energy of the sprung mass. Its momentum may not even be enough to move the spring.

Detailed analysis of individual cases is provided by the theory of vibrations.

The choice of the characteristics of the spring is determined by its purpose and the structure of the system into which it is integrated. For example, springs with supercritical characteristics are designed mainly for one-time action. Their characteristics resemble a plastic body, and their purpose is to fully dissipate the impact energy. Critical characteristics allow the system to return to its original state, but this is an ideal case, requiring some efficiency framework in design practice. Subcritical characteristics lead to forced vibrations of the systems, depending on the nature of the load. For example, in the case of a forced oscillation character, the selection of spring parameters requires the analysis of the amplitude-frequency characteristics of the system.

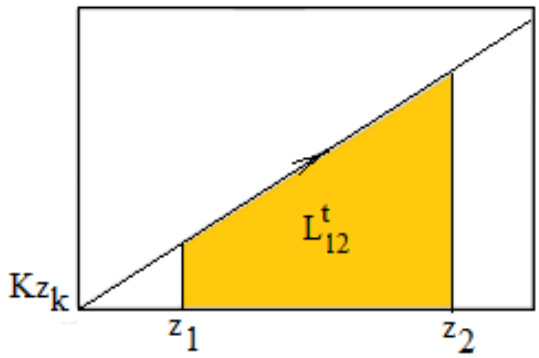

Fig. 16. Supercritical case without elastic return

The way to modify the characteristics of springs, apart from the mentioned geometric dimensions and friction coefficient, is to select the number of spring modules. With constant module's constructional parameters, increase of their number translates into increase of susceptibility, which is also influenced by nonlinear character of module's stiffness. At the same time, it causes multiplication of strain energy dissipation.

6. The results of the experiment

Figure 17 shows samples of mating pairs of rings. Figure 18 the test system for the characteristics of sample (a) and examples of sample characteristics (b).

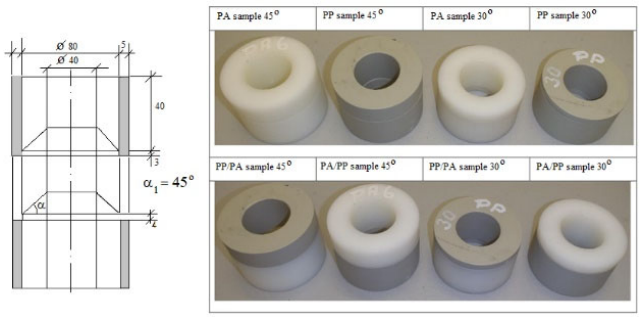

Fig. 17. Samples of mating pairs of rings; PA – polyamide, PP - polypropylene

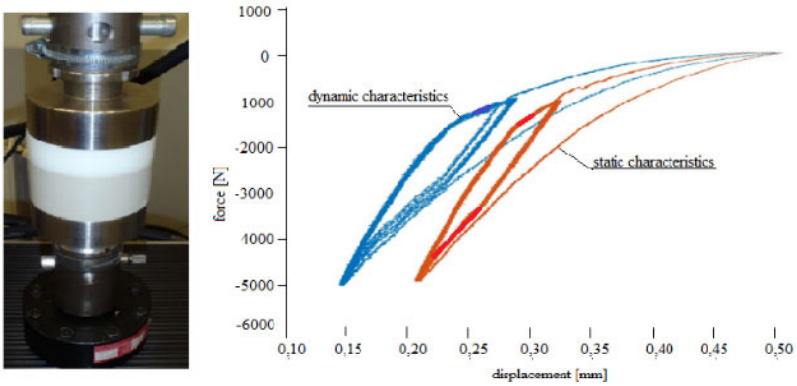

Fig. 18. The test system (a) and characteristics of the selected sample (b)

7. Conclusions

1. Annular springs are, structurally, an alternative to traditional design solutions – shape springs, band springs, flat springs, leaf springs, disc springs, wave springs, conical springs – and material solutions – steel sheet or spring wire, elastomers or polymer composites.
2. The working load range of ring springs is limited to compression.
3. The rings are loaded by external, distributed pressures on the conical surface causing circumferential and radial stresses, tensile for the outer rings and compressive for the inner rings.
4. The characteristic properties of annular springs are a high degree of strain equalization under loading conditions and the presence of friction on the contact surfaces of the conical rings.
5. The number of modules, the angle of the contact surface cone, the material or combination of materials, the surface properties can shape the compliance strength, the operating efficiency, which can be measured by the ability to retain or dissipate strain energy, depending on the function of the spring.
6. The advantage is preservation of functional ability despite damage of single modules.
7. The strength properties of polymers are significantly lower than the corresponding ones made of steel, which defines an alternative area of application.
8. The thermal properties of polymers, the low thermal conductivity and the temperature-load elastic limit, determine the area of application for slowly varying, pulsating loads with low irregularity or characterized by a limited ratio of dynamic and static load periods or Due to the total corrosion resistance, water cooling can be used.
9. Low modulus of elasticity indicates the possibility of application in compensation systems of mismatch in contact connections in rigid structures, as in construction or support systems or compensation of mismatch in modules of steel structures.
10. The ability to work under static preload conditions and resistance to machine oils and fats indicate the suitability for the foundation of machinery and industrial equipment, where vibration isolation capabilities are also beneficial.
11. Waste-free ring forming techniques are possible and recommended.
12. It is advisable to design and select design features of rings and springs, taking into account individual application requirements.

In the next publication, examples of modelling, analysis and design of ring springs corresponding to different functional conditions will be provided

References

[1] M. Radeş, Shock isolation systems, in: S. Brown (ed.), Encyclopedia of Vibration, Academic Press, Cambridge, MA, 2001, 1180-1184. DOI: https://doi.org/10.1006/rwvb.2001.0177

[2] Y. Ling, S. Wu, J. Gu, H. Lai, A Novel Ring Spring Vibration Isolator for Metro Superstructure, Applied Sciences 11/18 (2021) 8422. DOI: https://doi.org/10.3390/app11188422

[3] Z. Chao, Y. Wang, J.A. Moore, M. Sanayei, Train-induced field vibration measurements of ground and over-track buildings, Science of the Total Environment 575 (2017) 1339-1351. DOI: https://doi.org/10.1016/j.scitotenv.2016.09.216

[4] Z. Chao, Y. Wang, W. Peng, J. Guo, Measurement of ground and nearby building vibration and noise induced by trains in a metro depot, Science of the Total Environment 536 (2015) 761-773. DOI: https://doi.org/10.1016/j.scitotenv.2015.07.123

[5] C. Zou, J.A. Moore, M. Sanayei, Y. Wang, Impedance model for estimating train-induced building vibrations, Engineering Structures 172 (2018) 739-750. DOI: https://doi.org/10.1016/j.engstruct.2018.06.032

[6] M. Sitarz, W. Gamon, Railway buffers. Requirements. Design. Examinations. Part 1. Division of buffers, TTS Technika Transportu Szynowego 20/9 (2013) 29-35 (in Polish).

[7] Grimm, RINGFEDER friction ring springs, Technical description (in Polish). Available from: https://grim.pl/main_libs/files/assets/1/sprezyny_pierscieniowe_cierne/sprezyny-pierscieniowe-cierne.pdf

© 2022 by the authors. Licensee International OCSCO World Press, Gliwice, Poland. This paper is an open access paper distributed under the terms and conditions of the Creative Commons Attribution-NonCommercial-NoDerivatives 4.0 International (CC BY-NC-ND 4.0) license (https://creativecommons.org/licenses/by-nc-nd/4.0/deed.en).